A Journal of the Gesellschaft Deutscher Chemiker

Angewandte International Edition GDCh Chemie

www.angewandte.org

Accepted Article

Title: Robust Ultramicroporous Metal-Organic Frameworks with Benchmark Affinity for Acetylene

Authors: Yun-Lei Peng, Tony Pham, Pengfei Li, Ting Wang, Yao Chen, Kai-Jie Chen, Brian Space, Katherine Forrest, Peng Cheng, Zhenjie Zhang, and Michael Zaworotko

To be cited as: *Angew. Chem. Int. Ed.* 10.1002/anie.201806732
Angew. Chem. 10.1002/ange.201806732

Link to VoR: http://dx.doi.org/10.1002/anie.201806732
http://dx.doi.org/10.1002/ange.201806732

WILEY-VCH

10.1002/anie.201806732

WILEY-VCH

Robust Ultramicroporous Metal-Organic Frameworks with Benchmark Affinity for Acetylene

Yun-Lei Peng,[a] Tony Pham,[f] Pengfei Li,[d] Ting Wang,[a] Yao Chen,[e] Kai-Jie Chen,[b] Katherine A. Forrest,[f] Brian Space,[f] Peng Cheng,[a], [c] Michael J. Zaworotko,* [b] Zhenjie Zhang* [a], [c], [e]

Abstract: Highly selective separation and/or purification of acetylene from various gas mixtures is a relevant and difficult challenge which currently requires costly and energy intensive chemisorption processes. Herein, we demonstrate that two ultramicroporous metal-organic framework physisorbents, **NKMOF-1-M** (M = Cu or Ni), offer high hydrolytic stability and benchmark selectivity towards acetylene vs. several gases at ambient temperature. We attribute the performance of **NKMOF-1-M** to their exceptional acetylene binding affinity as revealed by modeling and several experimental studies: in situ single crystal X-ray diffraction and FT-IR; gas mixture breakthrough tests. **NKMOF-1-M** exhibit better low pressure uptake than existing physisorbents and possesses the highest selectivities yet reported for C_2H_2/CO_2 and C_2H_2/CH_4. This study introduces a new strategy for the design of porous materials for acetylene separation since the performance of **NKMOF-1-M** is not driven by the same mechanism as current benchmark physisorbents that rely on pore walls lined by inorganic anions.

Acetylene (C_2H_2) is not only an important fuel gas, but also an industrial commodity that is widely used for production of plastics (e.g. PVC and PVDF), acrylic derivatives, vinyl compounds, and α-ethynyl alcohols.[1] The production of C_2H_2 usually generates methane (CH_4) and carbon dioxide (CO_2) due to insufficient combustion of methane or the nature of the steam cracking process in petroleum refining.[2] Therefore, developing highly efficient and energy-efficient approaches to purify acetylene from C_2H_2/CH_4 and C_2H_2/CO_2 mixtures is of industrial relevance.[4-6] Besides the production of high purity C_2H_2, elimination of trace amounts of C_2H_2 is also of industrial importance. For instance, in polyethylene production acetylene is a trace contaminant that must be removed because it poisons the polymerisation catalyst by formation of solid metal acetylides that can block the fluid stream and even lead to explosions.[7] Currently, there are two major technologies to remove trace C_2H_2: (i) solvent extraction using a large volume of solvent (e.g. DMF or acetone); (ii) partial hydrogenation of C_2H_2 into ethylene using noble metal catalysts. These two approaches suffer from high cost and low efficiency,[8,9] so new strategies for separation/purification of C_2H_2 are needed.

Metal-organic frameworks (MOFs) can offer crystallinity, ultra-high surface area (>6000 m^2/g) and tunable pore size because of their compositional diversity, control over pore chemistry.[10] In the past two decades, MOFs have been studied with respect to gas storage[11-13] and/or separation,[14-22] catalysis,[23] drug delivery,[24] conductivity[25,26] and magnetism.[27-28] In principle, MOFs have the potential to supercede traditional porous materials such as zeolites, silica and activated carbon as they can be designed to offer features to enhance C_2H_2 capture: (i) open metal sites for strong interactions between C_2H_2 and pore walls, e.g. Long *et al.* reported that **MOF-74** materials exhibit high uptake of C_2H_2 and strong C_2H_2 separation selectivity thanks to a high density of open metal sites and large specific surface areas.[14] (ii) Functional groups (e.g. NH_2, SiF_6^{2-}, TiF_6^{2-} and $NbOF_5^{2-}$) on the pore walls of MOFs can afford strong sorbent-sorbate interactions.[29] For example, we recently reported that a member of the SIFSIX family of hybrid ultramicroporous materials, **SIFSIX-2-Cu-i**,[4,30] can exhibit benchmark C_2H_2/C_2H_4 and C_2H_2/CO_2 separation performance. The key feature of the **SIFSIX** family is the MF_6^{2-} (M = Si, Ti, etc) moiety which allows for strong sorbate-sorbent (F···HC≡CH···F interactions) with C_2H_2.[31] (iii) Tailored pore sizes can endow MOFs with a sieving effect. For instance, although **SIFSIX-14-Cu-i** (pore size: ~3.4 Å) exhibits high C_2H_2 uptake, it does not adsorb ethylene and it superceded **SIFSIX-2-Cu-i** with respect to C_2H_2/C_2H_4 selectivity.[32] Herein, we report two ultramicroporous MOFs (**NKMOF-1-M**, **M = Cu, Ni**) that offer a new type of binding site for C_2H_2 that results in the highest selectivities yet reported for C_2H_2/CO_2 and C_2H_2/CH_4.

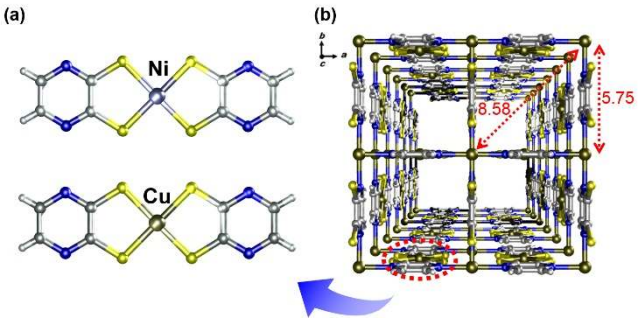

Figure 1. (a) The $[M(pdt)_2]^-$, M = Cu, Ni, metalloligands in **NKMOF-1-M**; (b) the crystal structure of **NKMOF-1-M** viewed along the *c* axis.

NKMOF-1-M (Cu[M(pdt)$_2$], M = Cu, Ni) materials are based on pyrazine-2,3-dithiol (pdt) and were prepared via previously reported procedures with slight modification.[24,33,34] Figure 1 reveals that **NKMOF-1-M** possess a 3D framework with one-dimensional (1D) square channels along the *c* direction. Cu or Ni ions exhibit 4-coordinate square planar geometry with four sulfur atoms to form 4-connected $[M(pdt)_2]^-$ (M = Cu, Ni) building units (Figure 1a) linked by 4-connected square planar Cu centers, to generate isostructural 4,4-connected **pts** topology networks. Cu,

[a] College of Chemistry, Nankai University, Tianjin, 300071, China.
[b] Department of Chemical Sciences, Bernal Institute, University of Limerick, Limerick V94T9PX, Republic of Ireland.
[c] Key Laboratory of Advanced Energy Materials Chemistry (MOE), Nankai University, Tianjin 300071, China.
[d] Department of Chemistry, HEBUST, Qinhuangdao 066004, China
[e] State Key Laboratory of Medicinal Chemical Biology, Nankai University, Tianjin 300071, China.
[f] Department of Chemistry, University of South Florida, 4202 East Fowler Avenue, CHE205, Tampa, Florida 33620-5250, United States.
Correspondence to: Zhenjie Zhang (zhangzhenjie@nankai.edu.cn), Michael J. Zaworotko (xtal@ul.ie)

Supporting information for this article is given via a link at the end of the document.

NKMOF-1-Cu, or Ni, **NKMOF-1-Ni**, atoms from $[M(pdt)_2]^-$ building units line the walls of the 1D channels which possess square pores of 5.75 Å (Cu···Cu distance after subtracting van der Waals radius) (Figure 1b). The combination of ultramicropores and open metal sites endow **NKMOF-1-M** with the potential for high C_2H_2 binding affinity.

The ubiquity and small kinetic diameter of water vapour means that sorbents must exhibit hydrolytic stability in order to have utility. **NKMOF-1-M** are stable in water for at least six months at room temperature or in pH = 1 or 12 water for one week as verified by PXRD and surface area measurements (Figure S1, S2 and S3). Variable temperature PXRD of **NKMOF-1-Ni** (Figure S4) revealed that it exhibits thermal stability to 240 °C whereas **NKMOF-1-Cu** loses crystallinity above 60 °C. In order to assess porosity of **NKMOF-1-M**, N_2 sorption isotherms were collected at 77K. **NKMOF-1-Ni** showed a typical type I isotherm and a BET surface area of 382 m^2/g after activation under vacuum at 90 °C without solvent exchange (Figure S5). **NKMOF-1-Cu** was activated using CO_2 supercritical drying and afforded a BET surface area of 280 m^2/g. Considering the less convenient activation conditions, lower thermal stability and lower BET surface area of **NKMOF-1-Cu**, **NKMOF-1-Ni** became the primary focus of further study.

Single-component adsorption isotherms for C_2H_2, C_2H_4, C_2H_6, CO_2, CH_4 and N_2 were collected for **NKMOF-1-Ni** at 273 K, 288 K and 298 K (Figure S6). **NKMOF-1-Ni** was found to adsorb 61.0 cm^3/g of C_2H_2, 47.3 cm^3/g of C_2H_4, 51.1 cm^3/g of CO_2, 33.5 cm^3/g of C_2H_6, 22.2 cm^3/g of CH_4 and 7.3 cm^3/g of N_2 at 1 bar and 298 K (Figure 2a and S6). Gas mixture selectivity generally correlates with the adsorption behavior of single-component gases in the low-pressure region. In **NKMOF-1-Ni**, we compared the adsorption capacity of each single component (C_2H_2, C_2H_4, CO_2 and CH_4) gas at low-pressure and 298 K (Figure 2a and 2b). **NKMOF-1-Ni** displayed strong uptake of C_2H_2 at low pressure. Indeed, C_2H_2 uptake of **NKMOF-1-Ni** is the highest (33.7 cm^3/g) yet observed at 0.003 bar and 298 K and can be compared with the current benchmark material **SIFSIX-14-Cu-i** (25.4 cm^3/g) (Figure 2c and Table S1). Although the surface area of **NKMOF-1-Cu** is lower than that of **NKMOF-1-Ni**, it also displayed a high uptake capacity of 25.8 cm^3/g (Figure 2c and S7) at 0.003 bar and 298 K. This exceptional C_2H_2 adsorption performance in the ultra-low-pressure region indicates strong C_2H_2-sorbent interactions in **NKMOF-1-M**. We focused further upon the following separations because of their practical relevance: C_2H_2/C_2H_4, C_2H_2/CO_2 and C_2H_2/CH_4.[4-7]

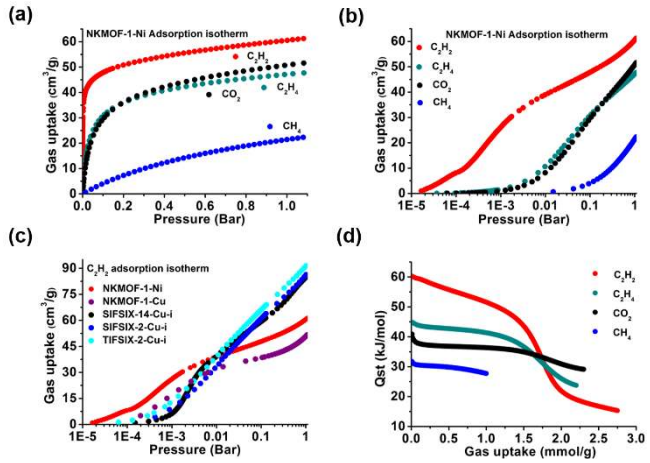

Figure 2. (a, b) Single-component gas adsorption isotherms of **NKMOF-1-M** at 298K; (c) C_2H_2 adsorption isotherms of various MOFs at 298 K; (d) Q_{st} of various gases for **NKMOF-1-M**.

The isosteric enthalpy of adsorption (Q_{st}) is a quantitative measure of the binding affinity of **NKMOF-1-Ni** towards C_2H_2, C_2H_4, CO_2, and CH_4. Q_{st} curves for various gases were calculated based on the single-component gas adsorption isotherms fitted with the dual-site-Langmuir-Freundlich isotherm model (Table S2, S3, S4 and S5). Q_{st} values were then calculated using Clausius-Clapeyron equation. The zero-coverage Q_{st} values of **NKMOF-1-Ni** are 60.3 kJ/mol, 44.9 kJ/mol, 40.9 kJ/mol and 31.7 kJ/mol for C_2H_2, C_2H_4, CO_2, and CH_4, respectively (Figure 2d). The dual-site-Langmuir-Freundlich (DSLF) method (Figure S8, Table S6) afforded similar results (C_2H_2: 53.9 kJ/mol for site I &19.0 kJ/mol for site II; C_2H_4: 40.9 kJ/mol; CO_2: 36.2 kJ/mol; CH_4: 28.5 kJ/mol). These Q_{st} values indicate that **NKMOF-1-Ni** offers potential to capture trace levels of C_2H_2 from various gas mixtures (e.g. C_2H_2/C_2H_4, C_2H_2/CO_2 and C_2H_2/CH_4).

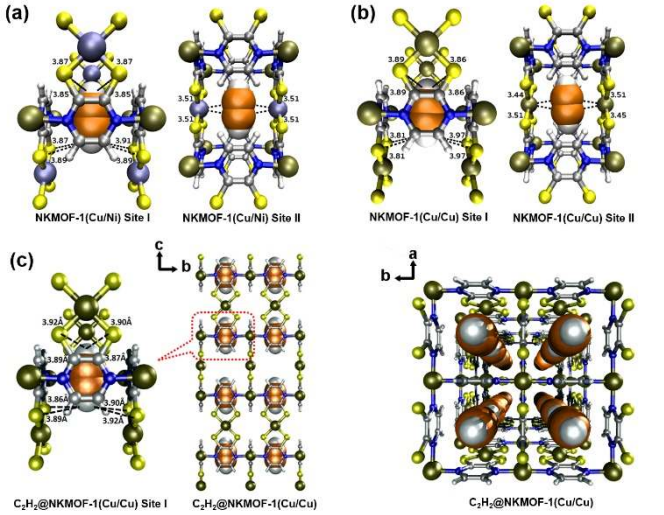

Figure 3. Two binding sites (I, II) of C_2H_2 determined via modeling studies conducted upon **NKMOF-1-Ni** (a) and **NKMOF-1-Cu** (b); single crystal structure of **C_2H_2@NKMOF-1-Cu** viewed along the *a* or *c* axis (c).

To understand the excellent acetylene adsorption performance of **NKMOF-1-M** we conducted detailed theoretical investigations using GCMC (Grand Canonical Monte Carlo) methods and first-principles DFT-D (dispersion-corrected density functional theory) calculations.[35,36] **NKMOF-1-M** exhibit two binding sites (I and II) for acetylene (Figure 3). The stronger site (Site I) combines hydrogen bonding (HC≡CH···S(MOF)) and π–π interactions between C_2H_2 and the pyrazine units in **NKMOF-1-M** (Figure 3a and 3b). The static adsorption energies were calculated to be 52.6 kJ/mol and 51.8 kJ/mol for **NKMOF-1-Ni** and **NKMOF-1-Cu**, respectively. The other binding site (Site II) is located in the middle of two open metal sites of adjacent MS_4 units (Figure 3a and 3b). Acetylene is usually weak alkaline, so it can readily be bound by Lewis acidic open metal sites (Cu, Ni). The static adsorption energies for these sites were calculated to be 25.2 kJ/mol and 30.3 kJ/mol for **NKMOF-1-Ni** and **NKMOF-1-Cu**, respectively. GCMC simulations indicate that saturation of C_2H_2 in **NKMOF-1-M** is achieved at 3.5 molecules per unit cell with 2 molecules at binding site I and 1.5 molecules at binding site II (Figure S9 and S10). The experimental data for C_2H_2

adsorption collected at 195 K (~3.1 molecules at 1 bar, Figure S11) agree well with the simulated result. Modelling data for C_2H_4 reveal similar binding sites (Figures S12 and S13). Site I is characterized by interactions between four ethylene hydrogen atoms and framework sulfur atoms. H···S interactions were also seen at Site II but with shorter interaction distances. Interestingly, the most favorable CO_2 adsorption site was observed at Site II, where the electronegative O atoms of the adsorbate interact favorably with the positively charged open-metal sites. Notably, the CO_2 orientation is perpendicular to both the channel and the two neighboring open-metal sites (Figure S14 and S15). We note that the distance across the channel is insufficient for favorable M···O=C=O···M interactions to occur in either structure. CO_2 molecules orient vertically in the center of the channel in a manner similar to that observed for acetylene at the same site, with both adsorbates primarily interacting with the pyrazine linkers. The modelled binding sites for CH_4 in **NKMOF-1-M** are similar to those for C_2H_2, C_2H_4, and CO_2 (Figure S16 and S17). The CH_4 molecule exhibits favorable interactions with the four surrounding pyrazine rings at site I in both MOFs.

The crystal structure of **NKMOF-1-Cu** under C_2H_2 (**C_2H_2@NKMOF-1-Cu**) was studied to determine binding sites. Activated **NKMOF-1-Cu** crystals suitable for single-crystal X-ray diffraction (SCXRD) were filled with C_2H_2 via a C_2H_2 balloon at room temperature and SCXRD data was collected at 120 K. C_2H_2 molecules with full site occupancy were located between the four pyrazine rings (Figure 3c), consistent with the strong binding site, site I, determined by modelling. C_2H_2 molecules form hydrogen bonds (HC≡CH···S) with the eight sulfur atoms and C-H···S distances range from 3.86 Å to 3.92 Å. No C_2H_2 molecules were found at the weaker binding site (II). This result indicates that C_2H_2 molecules preferentially bind to site I at lower pressures at room temperature (2 molecules per unit cell according to the modelling study). The experimental zero-coverage Qst should be therefore approximate the static adsorption energy of binding site (I). The experimental gas adsorption data for **NKMOF-1-Ni** revealed that **NKMOF-1-Ni** sorbed ~2 molecules of C_2H_2 per unit cell at 0.05 bar and 298 K, which we ascribed to adsorption at site I. The Q_{st} of **NKMOF-1-Ni** at site I calculated from experimental data (53.9 kJ/mol) is close to that determined by modelling. These results indicate **NKMOF-1-M** exhibits excellent C_2H_2 separation performance.

Adsorption selectivity is a critical factor to assess the separation performance for an adsorbent material.[37-39] We calculated the gas mixture selectivity of **NKMOF-1-M** using ideal adsorbed solution theory (IAST). As displayed in Figure 4a, the adsorption selectivities at 298 K were determined to be 1272.6, 346.5, 249.3, 272.5, 6409.1 and 4949.2 for C_2H_2/C_2H_4 (1/99, v/v), C_2H_2/C_2H_4 (1/9, v/v), C_2H_2/CO_2 (1/1, v/v), C_2H_2/CO_2 (2/1, v/v), C_2H_2/CH_4 (1/1, v/v) and C_2H_2/CH_4 (2/1, v/v), respectively. The selectivity of C_2H_2/C_2H_4 (1/99,v/v) is second only to **SIFSIX-14-Cu-i** (6320) (Table S1).[31] However, **NKMOF-1-Ni** offers benchmark selectivities with respect to four gas mixtures at room temperature: C_2H_2/CO_2 (1/1, v/v), C_2H_2/CO_2 (2/1, v/v), C_2H_2/CH_4 (1/1, v/v) and C_2H_2/CH_4 (2/1, v/v). The C_2H_2/CO_2 (1/1, v/v) selectivity of **NKMOF-1-Ni** (249.3) is more than an order of magnitude better than the current benchmark, **DICRO-4-Ni-i** (18.2).[4] The selectivity towards C_2H_2/CO_2 (2/1, v/v) of **NKMOF-1-Ni** (272.5) is also more than an order of magnitude better than **TIFSIX-2-Cu-i** (10.1), the current benchmark.[4] The selectivity towards C_2H_2/CH_4 (1/1, v/v) of **NKMOF-1-Ni** (6409.1) is more than an order of magnitude better than **ZJU-198a** (391.1) as reported by Qian *et al.*.[6]

To further examine the separation performance of **NKMOF-1-Ni**, experimental breakthrough experiments for C_2H_2/C_2H_4 (1/99, v/v), C_2H_2/C_2H_4 (1/9, v/v), C_2H_2/CO_2 (1/1, v/v), C_2H_2/CO_2 (2/1, v/v), C_2H_2/CH_4 (1/1, v/v) and C_2H_2/CH_4 (2/1, v/v) at 298 K were conducted (Figure 4). For C_2H_2/C_2H_4 (1/99, v/v) and C_2H_2/C_2H_4 (1/9, v/v), C_2H_2 breakthrough occurred at 243.0 min and 48.0 min, respectively, and the concentration of C_2H_2 is <1ppm before breakthrough (Figure S18). The purity of C_2H_4 (>99.9999%) exceeds the specification for industrial polymerization of ethylene. For C_2H_2/CO_2 (2/1, v/v) and C_2H_2/CO_2 (1/1, v/v), breakthrough of C_2H_2 occured after 10.5min and 35.1min, respectively. For C_2H_2/CH_4 (2/1, v/v) and C_2H_2/CH_4 (1/1, v/v) mixtures, breakthrough of C_2H_2 occurred at 17.6 min and 38.3 min, respectively. It is remarkable that the concentration of C_2H_2 is <1 ppm before C_2H_2 breakthrough (Figure S18). These results reveal that **NKMOF-1-Ni** selectively sorbs C_2H_2 in all tested conditions. In addition, we found that the breakthrough time correlates with the C_2H_2 concentration of each gas mixture; higher concentration of C_2H_2 leads to earlier C_2H_2 breakthrough. According to the breakthrough results, the selectivities of C_2H_2/C_2H_4 (1/99, v/v), C_2H_2/C_2H_4 (1/9, v/v), C_2H_2/CO_2 (2/1, v/v), C_2H_2/CO_2 (1/1, v/v), C_2H_2/CH_4 (2/1, v/v) and C_2H_2/CH_4 (1/1, v/v) are 43.6, 7.6, 1.8, 2.6, 8.8 and 6.6, respectively. Activated **NKMOF-1-Ni** powders were exposed to C_2H_2 gas mixtures at room temperature. Fourier Transform Infrared Spectroscopy (FT-IR) of **NKMOF-1-Ni** (Figure S19) demonstrated the characteristic stretching vibration of C_2H_2 at 3236.8 cm^{-1} and 734.8 cm^{-1}. No signals for C_2H_4, CH_4 and CO_2 were detected, further validating high binding affinity towards C_2H_2 by **NKMOF-1-Ni**. Finally, **NKMOF-1-Ni** can be recycled at least five times (Figure S20 and S21).

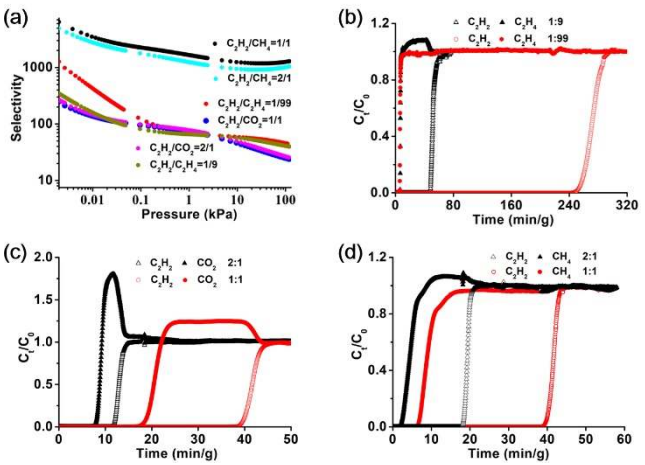

Figure 4. IAST adsorption selectivities (a) and breakthrough curves (b, c, d) of various C_2H_2 gas mixtures at 298K for **NKMOF-1-Ni**.

In conclusion, we report that an ultramicroporous MOF, **NKMOF-1-Ni**, exhibits excellent water stability over a broad pH range and new benchmarks for C_2H_2/CO_2 and C_2H_2/CH_4 selectivity by more than an order of magnitude *vs.* current benchmark materials. Overall, **NKMOF-1-Ni** exhibits four new benchmark selectivity values: C_2H_2/CO_2 (1/1), C_2H_2/CO_2 (2/1), C_2H_2/CH_4 (1/1) and C_2H_2/CH_4 (2/1). We attribute the superior performance of **NKMOF-1-Ni** to a new type of specific binding site for C_2H_2 as verified by modelling and *in situ* SCXRD. This

work not only provides a new approach to the design of porous materials with strong binding affinity for C_2H_2, but also promotes MOF physisorbent materials with potential to resolve industrial challenges related to C_2H_2 separation.

Acknowledgements

The authors acknowledge the support of National Natural Science Foundation of China (21601093), Science Foundation Ireland (13/RP/B2549 and 16/IA/4624), National Science Foundation of US (Awards DMR-1607989, CHE-1531590), XSEDE Grant of US (No.TG-DMR090028) and American Chemical Society Petroleum Research Fund grant (ACS PRF 56673-ND6).

Keywords: Metal-organic frameworks, ultramicroporous materials, acetylene separation, gas breakthrough, acetylene binding site, hydrolytic stability

[1] P. Pässler, W. Hefner, K. Buckl, H. Meinass,H.-J. Wernicke, G. Ebersberg, R.Müller, J. Bässler, H. Behringer, D. Mayer, Ullmann's Encyclopedia of Industrial Chemistry. Wiley-VCH: Weinheim, Germany, **2000**.

[2] A. Granada, S. B. Karra, S. M. Senkan, *Eng. Chem. Res.* **1987**, *26*, 1901-1905.

[3] R. Matsuda, R. Kitaura, S. Kitagawa, Y. Kubota, R. V. Belosludov, T. C. Kobayashi, H. Sakamoto, T. Chiba, M. Takata, Y. Kawazoe, Y. Mita, *Nature* **2005**, *436,* 238-241.

[4] K.-J. Chen, H. S. Scott, D. G. Madden, T. Pham, A. Kumar, A. Bajpai,M. Lusi, K. A. Forrest, B. Space, J. J. Perry IV, M. J. Zaworotko, *Chem* **2016**, *1*, 753-765.

[5] F. Luo, C. S. Yan, L.L. Dang, R. Krishna, W. Zhou, H Wu, X. L. Dong, Y. Han, T.-L. Hu, M. O'Keeffe, L. L. Wang, M. B. Luo, R.-B. Lin, B. L. Chen, *J. Am. Chem. Soc.* **2016**, *138*, 5678-5684.

[6] L. Zhang, X. L Cui, H. B. Xing, Y. Yang, Y. J. Cui, B. L. Chen, G. D. Qian, *RSC Adv.* **2017**, *7*, 20795-20800.

[7] H. Molero, B. F. Bartlett, W. T. Tysoe, *J. Catal.* **1999**, *181*, 49–56.

[8] J. D. Lewis, US Patent. 3, Separation of acetylene from ethylene-bearing gases. **1974**, *837*, 144.

[9] Z. B. Bao, G. G. Chang, H. B. Xing, R. Krishna, Q. L. Ren, B. L. Chen, *Energy Environ. Sci.* **2016**, *9*, 3612-3641.

[10] P. Li, N. A. Vermeulen, C. D. Malliakas, D. A. Gómez-Gualdrón, A. J. Howarth, B. L. Mehdi, A. Dohnalkova, N. D. Browning, M. O'Keeffe, O. K. Farha, *Sicence* **2017**, *356*, 624-627.

[11] J. A. Mason, M. Veenstrab, J. R. Long, *Chem. Sci.* **2014**, *5*, 32-51.

[12] C. -C. Liang, Z. -L. Shi, C. -T. He, J. Tan, H. -D. Zhou, H. -L. Zhou, Y. J. Lee, Y.-B. Zhang, *J. Am. Chem. Soc.* **2017**, *139,* 13300-13303.

[13] C. A. Trickett, A. Helal, B. A. Al-Maythalony, Z. H. Yamani, K. E. Cordova, O. M. Yaghi, *Nat. Rev. Mater.* **2017**, *2*, 1-16.

[14] E. D. Bloch, W. L. Queen, R. Krishna, J. M. Zadrozny, C. M. Brown, J. R. Long, *Science* **2012**, *335*, 1606-1610.

[15] P. Nugent, Y. Belmabkhout, S. D. Burd, A. J. Cairns, R. Luebke, K. Forrest, T. Pham, S. Q. Ma, B. Space, L. Wojtas, M. Eddaoudi, M. J. Zaworotko, *Nature* **2013**, *495*, 80-84.

[16] A. Cadiau, K. Adil, P. M. Bhatt, Y. Belmabkhout, M. Eddaoudi, *Science* **2016**, *353*, 137-140.

[17] K. Adil, Y. Belmabkhout, R. S. Pillai, A. Cadiau, P. M. Bhatt, A. H. Assen, G. Maurin, M. Eddaoudi, *Chem. Soc. Rev.* **2017**, *46*, 3402.

[18] P.-Q. Liao, N.-Y. Huang, W.-X. Zhang, J.-P. Zhang, X.-M. *Science* **2017**,*356*, 1193-1196.

[19] P.-Q. Liao, W.-X. Zhang, J.-P. Zhang, X.-M. Chen,*Nature Communications*, **2015**, 6, 8697.

[20] P.-Q. Liao, H. Chen, D.-D. Zhou, S. Y. Liu, C.-T. He, Z. Rui, H. Ji, J.-P. Zhang, X.-M. Chen, *Energy Environ. Sci.* **2015**, *8*, 1011-1016

[21] J.-P. Zhang, A.-X Zhu, R.-B. Lin, X.-L. Qi, X.-M. Chen, *Adv. Mater*, **2011**, *23*, 1268–1271.

[22] J.-P. Zhang, X.-M. Chen, *J. Am. Chem. Soc.* **2009**, *131*, 5516-5521.

[23] Y.-B. Huang, J. Liang, X.-S. Wang, R. Cao, *Chem. Soc. Rev.* **2017**, *46*, 126.

[24] Z. Y. Dong, Y. Z. S. Sun, J. Chu, X. Z. Zhang, H. X. Deng, *J. Am. Chem. Soc.* **2017**, *139*, 14209-14216.

[25] Y. Kobayashi, Benjamin. Jacobs, M. D. Allendorf, J. R. Long, *Chem. Mater.* **2010**, *22*, 4120-4122.

[26] J. -H. Dou, L. Sun, Y. C. Ge, W. B. Li, C. H. Hendon, J. Li, S. Gul, J.Yano , E. A. Stach, M. Dincă, *J. Am. Chem. Soc.* **2017**, *139*, 13608-13611.

[27] D. A. Reed, B. K. Keitz, J. Oktawiec, J. A. Mason, T. Runčevski, D. J. Xiao, L. E. Darago, V. Crocellà, S. Bordiga, J. R. Long, *Nature* **2017**, *550*, 96-102.

[28] H. C. Hendon, J. A. Rieth, D. M. Korzyński, M. Dinca, *ACS Cent. Sci.* **2017**, *3*, 554-563.

[29] T. -L. Hu, H. L. Wang, B. Li, R. Krishna, H. Wu, W. Zhou, Y. F. Zhao, Y. Han, X. Wang, W. D. Zhu, Z. Z. Yao, S. C. Xiang, B. L. Chen, *Nat. Commun.* **2015**, *6,* 7328.

[30] A. Bajpai, D. O'Nolan, D. G. Madden, K.-J. Chen, T. Pham, A. Kumar, M. Lusi, J. J. Perry, IV, B. Space M. J. Zaworotko, *Chem. Commun.* **2017**, *53*, 11592-11595.

[31] X. Cui, K. Chen, H. Xing, Q. Yang, R.Krishna, Z. Bao, H. Wu, W. Zhou, X. Dong, Y Han, B Li, Q Ren, M. J. Zaworotko, B. Chen, *Science* **2016**, *353*, 141-144.

[32] B. Li ,X. Cui, D. O'Nolan, H.-M. Wen, M. Jiang,R. Krishna, H. Wu, R.-B. Lin,Y.-S. Chen, D. Yuan, H. Xing, W. Zhou, Q. Ren, G. Qian, M. J. Zaworotko, B. Chen, *Adv. Mater.* **2017**, *29*, 1704210.

[33] J.-W. Xiu, G.-E Wang, M.-S. Yao,a C.-C. Yang, C.-H. Lin, G. Xu, *Chem. Commun.* **2017,** 53, 2479.

[34] S. Takaishi, M. Hosoda, T. Kajiwara, H. Miyasaka, M. Yamashita, Y. Nakanishi, Y. Kitagawa, K. Yamaguchi, A. Kobayashi, H. Kitagawa, *Inorg. Chem.* **2009**, *48*, 9048-9050.

[35] N. Metropolis, A. W. Rosenbluth, M. N. Rosenbluth, A. H. Teller J. *Chem. Phys.***1953,** *21*, 1087-1092.

[36] S. Grimme, *J. Comput. Chem.* **2006**, *27*, 1787-1799.

[37] R. Krishna, B. Smit, S. Calero, *Chem. Soc. Rev.* **2002**, *31*, 185-194

[38] B. Liu, B. Smit, *Langmuir* **2009**, *25*, 5918-5926.

[39] J. Duan, M. Higuchi, R. Krishna, T. Kiyonaga, Y. Tsutsumi, Y. Sato, Y. Kubota, M. Takata, S. Kitagawa, *Chem. Sci.* **2014**, *5*, 660-666.

10.1002/anie.201806732

WILEY-VCH

Text for Table of Contents

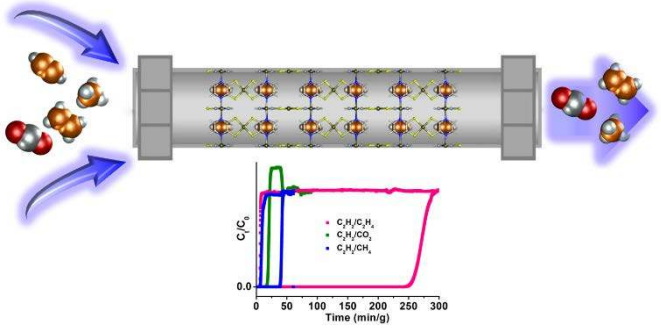

Yun-Lei Peng, Tony Pham, Pengfei Li, Ting Wang, Yao Chen, Kai-Jie Chen, Katherine A. Forrest, Brian Space, Peng Cheng, Michael J. Zaworotko, Zhenjie Zhang,**

Page No. – Page No.

Robust